[redacted] 134

[redacted]

UNCLASSIFIED

INVENTORIED
NOV 1 4 1962
3441-1

INVENTORIED
JUN 1 1 1957
BY ORG. 2743

SC-2969(TR)

COPY A

[redacted]

MAY 2 8 1985 WS

HIGH-ALTITUDE EFFECTS ON BLAST-THERMAL PARTITION OF ENERGY FROM NUCLEAR EXPLOSIONS, AND ASSOCIATED SCALING LAWS

F. H. Shelton, 5111

September 15, 1953

INVENTORIED
FEB 1 5 1968
3428-3

INVENTORIED
DATE 1-12-69

Return to:
CENTRAL FILE 7221-2
REPORTS REFERENCE

INVENTORIED
OCT 7 1964
3427-1

[redacted]

[redacted]

[redacted]

SANDIA SYSTEMATIC DECLASSIFICATION REVIEW
W.C. Loyne
97SU394
1-14-97

6-12-29
CCRP-RR
1-14-97
W Loyne
unclassified

Sandia Corporation
CONTRACTORS FOR U.S. ATOMIC ENERGY COMMISSION
ALBUQUERQUE • NEW MEXICO

INVENTORIED
DATE 11-11-61

1320 CENTRAL FILE

UNCLASSIFIED

[redacted]

[redacted]

ABSTRACT

High-altitude effects on blast-thermal partition of energy from nuclear explosions are calculated up to altitudes of 100-thousand feet. With increasing altitude, the amount of thermal energy increases and the blast energy decreases.

Below 50-thousand feet, altitude effects on the partition of energy are negligible. For example, a 1-KT weapon detonated at 50-thousand feet has the lethal gust radius for a B-29 type craft decreased only 30 feet and the lethal thermal radius increased 45 feet due to the departure in the partition of energy from sea-level conditions.

Above 50-thousand feet, the variation in partition of energy becomes increasingly important. For weapons larger than 10 KT, this results in the lethal thermal radius for a B-29 type craft exceeding the lethal gust radius.

SC-2969

TABLE OF CONTENTS

LIST OF ILLUSTRATIONS

SC-2969

HIGH-ALTITUDE EFFECTS ON BLAST-THERMAL PARTITION OF ENERGY FROM NUCLEAR EXPLOSIONS, AND ASSOCIATED SCALING LAWS

A detailed theoretical description of the detonation of a hypothetical 20-KT weapon under sea-level atmospheric conditions has been published[1] in which early growth of the fireball and formation and breakaway of the shock wave are treated. The amount of thermal radiation during this early phase of fireball growth (prior to breakaway of the shock wave) has been calculated for this 20-KT weapon by Magee and Hirschfelder.[2] From this analysis it is possible to determine the thermal radiation emitted by a high-altitude detonation, and a method of approximation is presented here whereby corresponding values of pertinent parameters may be derived for various altitudes ranging as high as 100-thousand feet. It should be stressed, however, that these derived results can be only qualitative since phenomena that may safely be neglected under sea-level burst conditions become significant at higher altitudes; for example, the mean free path of radiation through the shock front is a function of the density and temperature of the shock front, and consequently the magnitude of the loss of energy through thermal radiation from the interior of the fireball should be re-examined at each significant change in altitude.

But before discussing the method of approximation as applied to high-altitude detonations, it is perhaps best to review briefly the manner of growth of the fireball and the subsequent development of the shock wave for a representative detonation at an altitude in the vicinity of sea level. The following is essentially a recapitulation of the description given in The Effects of Atomic Weapons.* When the case of the weapon is dissolved, temperatures are of the order of one million degrees centigrade [2.6] and energy transport is by radiation. During this phase of fireball growth, which continues until the sphere has attained a radius of about 45 feet [2.7], the ambient air at a given point outside the periphery of the fireball sphere is heated to a high temperature by thermal radiation before the fireball itself would reach this point in the course of its normal hydrodynamic motion. By the time the fireball has attained a radius of about 45 feet, it will have engulfed a mass of air weighing 13,350 kg. If this mass is large compared to the mass of

---

*The referenced sections in The Effects of Atomic Weapons are indicated in the text of this paper in square brackets.

the bomb the equations of state of air are applicable. During this period the temperature of the fireball reaches its maximum, but it then drops rapidly as a result of expansion of the fireball and addition of new material. It is significant, too, that the pressure, temperature, and density of the air throughout the interior of the fireball are constant at any instant during this phase because of the long mean free paths of radiation inside the sphere [2.8].

When the radius of the sphere is approximately 45 feet, however, the velocity of hydrodynamic motion becomes greater than the velocity of radiation transport. The ambient air is engulfed by a shock front having a calculated pressure of about 80-thousand atmospheres [2.5 and Hirschfelder-Curtiss[8] data]. The air immediately behind the shock front has a temperature of 300,000°C [2.9], is highly ionized, and radiates. Thus beyond the 45-ft radius the shock front and the apparent surface of th fireball coincide, and the temperature at this surface is determined by the shock strength. Inside this sphere of shock-heated air is the original very hot isothermal sphere which has grown in size but is nearly the original fireball that engulfed the ambient air by radiation transport [6.11]. But because the shock-heated air is radiating it must be absorbing radiation, with the result that it is opaque to transmission of radiation from its interior. Viewed from a distance, the radiation appears to come from the surface of the fireball, and the distribution of its wavelengths is probably determined by the temperature of the shock-heated air [6.5]. Radiation ($\lambda >$ 1,860 Å) [6.14] from the shock front itself escapes through the transparent ambient air and dissipates energy from the shock front. This phase of fireball growth continues until the shock front no longer heats to incandescence the air through which it moves. The Taylor similarity conditions[3] indicate that during this phase the pressure of the shock front and the apparent temperature of the fireball have been decreasing as R^{-3}.

SC-2969

When the shock front has reached a distance of about 300 feet from burst zero, the air behind it is no longer radiant and the fireball of radiant air is left behind [2.11] -- in other words, the shock wave 'breaks away' from the fireball. Conditions in the vicinity of breakaway[7] are illustrated in Fig. 1. The surface temperature of the fireball is at a minimum in the vicinity of breakaway, and a layer of NO_2, HNO, and other nitrogen compounds forms which is opaque to radiation from the interior [6.10]. Thus radiation from the fireball to distant points decreases to a pronounced minimum at this time.

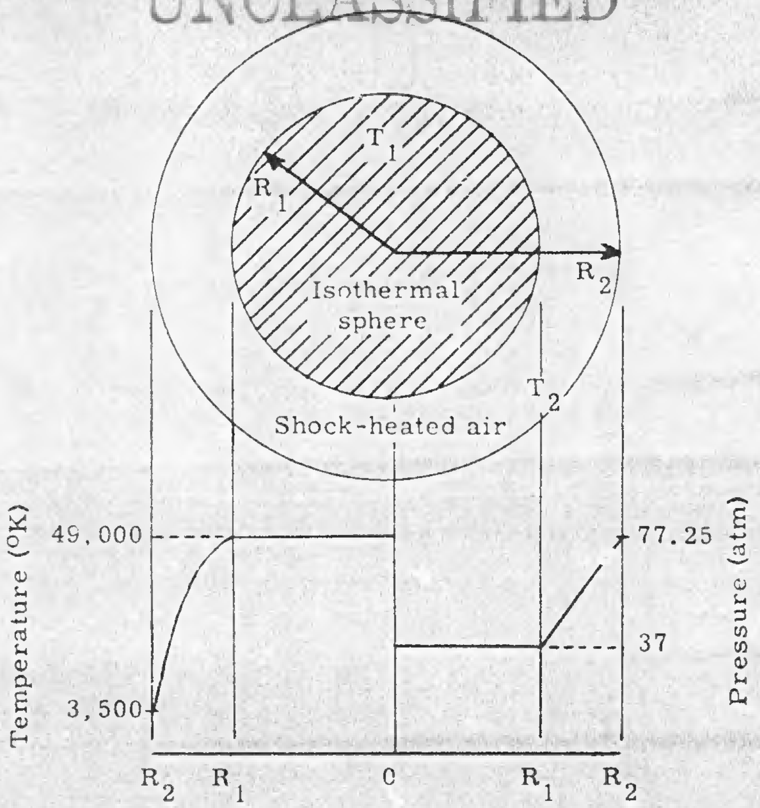

SC-2969

Conditions of the shock front:
R_2 = 330 feet
Pressure = 77.25 atmospheres
Temperature = 3,500°K
Density = 7.24 x ambient

Conditions of the isothermal sphere
R_1 = 220 feet
Pressure = 37 atmospheres
Temperature = 49,000°K
Density = 0.0392 x ambient

Fig. 1 -- Breakaway conditions at sea level for a 20-KT weapon

Total radiation between the first maximum* and this minimum is estimated to be of the order of 1 per cent of the radiochemical yield of the weapon [2.14]. Although wavelengths greater than 3000 Å are the only ones observed at large distances during this phase, wavelengths between 1,860 and 3000 Å are transmitted to distances sufficiently great that they may be considered lost during growth of the fireball. The author has calculated that somewhat less than 1 per cent of the radiochemical yield of the weapon escapes as thermal radiation from the fireball during the period between zero time and the first minimum of fireball intensity.

When estimates are made of the percentage of the yield emitted as radiation during this same phase at higher altitudes, it is found that this percentage will increase with

*The maximum temperature reached during early growth of the isothermal sphere.

elevation until at 100-thousand feet perhaps 50 times as much radiation will be emitted as at sea level for the same radiochemical yield. Because energy radiated during this phase of shock-wave formation is extracted from the energy of the shock front, the effective yield of the weapon is seriously reduced so far as blast damage is concerned although thermal effects are increased.

After breakaway there is transparent air immediately behind the shock front. The hot interior heats the surface of the fireball, and from a burst at sea level the bulk of the radiation is emitted at this time as a long-duration pulse. It is possible that at very high altitudes this phase of the radiation may take place very promptly, seriously depleting the energy in the shock wave, which is in the immediate vicinity of the fireball at this point. The mechanism by which this energy reduction takes place is thought to be a premature formation of the negative phase as a result of the rapid decrease in temperature of the extremely tenuous fireball.

To obviate the complicated detailed analysis required to arrive at the actual partition between thermal radiation and blast energy at various burst heights, it was evident that an approximation procedure should be devised. Such an approximation procedure could be applied at various altitudes

1. To determine to what altitudes known conditions at sea level can, with validity, be scaled and

2. When deviations from the partition of energy at sea level are small, to obtain nearly correct scaled conditions for the new altitude.

At very high altitudes there is a serious deviation in energy partition from that at sea level. Therefore, at higher altitudes, to obtain the actual time dependence and amount of thermal radiation and the blast efficiency of the weapon, the problem would have to be reconsidered and allowance made for a large radiation flux during fireball expansion. This large flux is a significant departure from the condition at sea level, where the amount of energy escaping the fireball prior to breakaway can be neglected and solution of the hydrodynamic equations simplified by assuming $\frac{d}{dt}$ (energy) = 0. At higher altitudes it will be necessary to include the term for radiation flux, F, in the fundamental equation,

$$\frac{d}{dt}\,(\text{energy}) = F,$$

with the result that the exact solution may be difficult to carry out on IBM machines. The problem would be treated by the Monte-Carlo method.

[redacted]

An exact solution at high altitudes would also involve an investigation of the equation of state for air as derived for a sea-level detonation. Perhaps extensions of this work are necessary for the low densities encountered at higher altitudes. The original work of Fuchs and Peierls[4] on the equations of the state for air should be studied in the light of their statement that "These errors have not yet been corrected in all results for the entropy and [the] adiabatics...are subject to corrections at very low densities." An accurate determination of the blast and thermal energies from a weapon detonated at a high altitude would involve a considerable expenditure of effort.

The Approximation Procedure

It is reasonable to assume that thermal radiation per unit area is determined by the temperature of the surface of the fireball. What is desired is a scaling law for radius and time for a given temperature of the fireball surface. Scaling is, of course, to be applicable at various ambient conditions. Then, whatever the radiative process at sea level, so long as the total radiation is known, we know, at the higher altitude, the radius of the fireball (and hence its total area) and how time scales for each temperature of the fireball at sea level. When the absolute temperature and radius of the fireball at sea level are T_o and R_o, it is radiating at the rate

$$\frac{dq_o}{dt_o} = f_o \, \sigma T_o^4 \, 4\pi R_o^2, \qquad (1)$$

where f_o is the fraction of the radiation spectrum transmitted by the ambient air, and σ is the Stefan-Boltzmann constant. It has been found experimentally that radiation of wavelengths less than about 1, 860 Å is not transmitted to any significant distance by the ambient air at sea level.[5] At higher altitudes it is possible that radiation of lesser wavelengths may be transmitted, but this transmission should be a weak function of altitude. Thus when the fireball at the higher altitude is also at the temperature T_o, it is radiating at the rate

$$\frac{dq_H}{dt_H} = f_{oH} \, \sigma T_o^4 \, 4\pi R_H^2 \, . \qquad (2)$$

Equations 1 and 2 may be combined to give

$$\frac{dq_H}{dq_o} = \frac{f_{oH} \, \sigma T_o^4 \, 4\pi R_H^2 \, dt_H}{f_o \, \sigma T_o^4 \, 4\pi R_o^2 \, dt_o} = \frac{R_H^2 \, dt_H}{R_o^2 \, dt_o} \qquad (3)$$

In equating f_{oH} and f_o it is possible that we are underestimating the actual radiation at higher altitudes in view of the increased transparency of the atmosphere.

From Eq 3 we obtain

$$\frac{\int_0^{Q_H} dq_H}{\int_0^{Q_o} dq_o} = \frac{Q_H}{Q_o} = \frac{\int_0^{t_H} R_H^2 dt_H}{\int_0^{t_o} R_o^2 dt_o} \tag{4}$$

where we interpret dt_H and dt_o as the times between the same differential temperatures at the higher altitude and sea level. The radiated energy (Q_H or Q_o) is that emitted from the shock front while the shock front and apparent surface of the fireball coincide.

To approximate the ratio of the energy radiated at any altitude, H, and sea level it will be sufficient to know how to scale distance and time for a given absolute temperature of the shock front. The scaling will be obtained from a consideration of the strong shock relations.

SC-2969

Shock Relations for Strong Shocks

Pressures and temperatures in the initial phase of a nuclear detonation are extremely high. Therefore the Rankine-Hugoniot shock relations[6] are re-examined here with the object of incorporating any reasonable approximations to obtain simpler equations appropriate to strong shock theory. These relations will be further transformed so that they may be stated in terms of only one ambient variable, the ambient density at the altitude in question. This is essentially the small $\gamma - 1$ theory that has been carried out before.[7]

<u>Shock Density</u>. -- The density, ρ_s, of the air behind the shock front, stated in terms of the ambient density, ρ_a, at a particular altitude is

$$\frac{\rho_s}{\rho_a} = \frac{\mu + \xi}{1 + \mu\xi} \tag{5}$$

where

$$\mu = (\gamma + 1)/(\gamma - 1)$$

$$\xi = P_a/P_s$$

γ = the 'effective' specific heat ratio for the air behind the shock front

P_a = the ambient air pressure

P_s = the absolute pressure of the shock front.

Since the pressure of the shock front in the fireball expansion phase of shock development is between 80, 000 and 80 atmospheres, the term ξ is very small

$$1/80,000 \leq \xi \leq 1/80 << 1$$

and can be neglected as compared with unity. Using such an approximation, Eq 5 becomes

$$\frac{\rho_s}{\rho_a} = \frac{\gamma + 1}{\gamma - 1} . \tag{6}$$

If the γ of the air behind the shock front were constant, the density of the shock front, ρ_s, would be a constant at a given altitude. But since γ is a variable for very high pressures and temperatures, the density of the shock front does change as the shock front propagates.

Absolute Temperature of the Shock Front. -- The absolute temperature, T_s, of the shock front, stated in terms of the ambient temperature, T_a, is

$$\frac{T_s}{T_a} = \frac{1 + \mu\xi}{(\mu + \xi)\xi} . \tag{7}$$

Using the approximation that ξ is small,

$$\frac{T_s}{T_a} = \frac{1}{\mu\xi} \tag{8}$$

or

$$\frac{T_s}{T_a} = \frac{P_s}{P_a} \frac{\gamma - 1}{\gamma + 1} = \frac{P_s \rho_a}{P_a \rho_s} , \tag{9}$$

and

$$T_s = \frac{T_a P_s (\gamma - 1)}{P_a (\gamma + 1)} = \frac{\overline{M} P_s (\gamma - 1)}{G \rho_a (\gamma + 1)} . \tag{10}$$

For the ambient air ahead of the shock we can use $T_a/P_a = \overline{M}/G\rho_a$, where G is the universal gas constant, and $\overline{M}$ is the average molecular weight of air.

It will be shown (Eq 15) that

$$T_s = \frac{\overline{M}}{G} \frac{2(\gamma - 1)}{(\gamma + 1)^2} \dot{R}^2$$

where $\dot{R}$ is the velocity of the shock front. Equation 15 will prove to be important in the later development of the scaling theory. Ambient conditions do not appear in this equation. In reviewing the above equation it is seen that the absolute temperature of the shock front is proportional to $\dot{R}^2$. Since γ is principally a function of temperature, Eq 15 is very nearly independent of altitude, and whenever the shock velocities are the same, the absolute temperature of the air behind such shock fronts is the same.

The Shock Velocity, $\dot{R}$

$$\frac{\dot{R}}{c} = \sqrt{\frac{\mu + \xi}{(1 + \mu)\xi}} , \tag{11}$$

where c is the velocity of sound in the ambient air ahead of the shock front. Squaring Eq 11 we obtain

$$\dot{R}^2/c^2 = (\mu + \xi)/(1 + \mu)\xi = P_s(\gamma + 1)/2\gamma P_a . \tag{12}$$

For the velocity of sound in the ambient air we substitute

$$c^2 = \frac{\gamma_o P_a}{\rho_a}$$

and obtain, with the approximation that $\gamma_o = \gamma$,

$$\frac{P_s}{\rho_a} = \frac{2}{\gamma + 1} \dot{R}^2 . \tag{13}$$

Solving for P_s/ρ_a (Eqs 10 and 13),

$$\frac{P_s}{\rho_a} = \frac{GT_s(\gamma + 1)}{\overline{M}(\gamma - 1)} = \frac{2}{\gamma + 1} \dot{R}^2 , \tag{14}$$

and the absolute temperature of the shock front, T_s, is

$$T_s = \frac{2\overline{M}(\gamma - 1)}{G(\gamma + 1)^2} \dot{R}^2 . \tag{15}$$

Pressure Distribution Inside the Isothermal Sphere. -- Although the derivation is quite lengthy, one can show in a rather straightforward manner that the pressure at R = 0 is $P_s/2$; that is the pressure in the isothermal sphere is half that of the shock front after the shock velocities are greater than the rate of radiation transport.

SC-2969

[redacted]

$$P(0) = P_s/2 . \tag{16}$$

Returning to the breakaway conditions (Fig. 1) it is seen that the pressure of the isothermal sphere is nearly half the pressure at the shock front [3, 6].

<u>The Total Energy, W, within the Sphere Encompassed by the Shock Front.</u> -- When the shock front is at a distance R from burst zero and has a pressure P_s, the total internal energy of the gas enclosed within the shock front is

$$W(R) = \int_{Vol} \frac{P}{\gamma - 1}\, dV = \frac{P_s}{2} \frac{1}{\gamma - 1} \frac{4}{3} \pi R^3 , \tag{17}$$

where Eq 16 was used as the average pressure over the volume. Substituting for the shock pressure, P_s, the expression derived from Eq 13, we obtain

$$W(R) = \frac{\rho_a}{2} \frac{1}{\gamma - 1} \frac{4}{3} \pi R^3 \dot{R}^2 \tag{18}$$

if γ is taken to be nearly 1($\sim$ 1.2) and $\gamma + 1$ as nearly 2. Although a number of approximations have been made in deriving Eqs 17 and 18, these equations are essentially correct for the total energy (internal and kinetic) within the shock front because of a compensation of errors as pointed out by Bethe:[7] "It is, of course, only an accident that there is almost exact compensation of all those neglected terms up to values of γ as high as 5/3." The kinetic energy is $\gamma - 1$ times the internal energy, and for γ's near 1 the kinetic energy is relatively small. Equations 17 and 18 are nearly correct despite radiation of energy from the shock front because P(0) will remain nearly that determined by a nonradiating shock front. If only a small amount of energy has been emitted during the phase from zero time to the first minimum, the radiochemical yield of the weapon is used for W(R).

SC-2969

<u>Time of Arrival of the Shock Front at Radius R</u>

When variables are separated, Eq 18 gives

$$R^{3/2}\, dR = \sqrt{\frac{3W(\gamma - 1)}{2\pi\rho_a}}\, dt . \tag{19}$$

If the energy, W, is a constant, integration leads to

$$\frac{2R^{5/2}}{5} = \sqrt{\frac{3W(\gamma - 1)}{2\pi\rho_a}}\, t , \tag{20}$$

[redacted]

or

$$t = \frac{2}{5}\sqrt{\frac{2\pi\rho_a}{3W(\gamma - 1)}}\, R^{5/2}.$$

Scaling of Radii and Times at Various Altitudes for the Same Absolute Temperature of the Shock Front

From Eq 15 it is seen that the absolute temperature, T_s, immediately behind the shock front is the same for shock fronts having equal velocities. Using Eq 18 and requiring that the absolute temperatures be equal, it is found that the radii scale as

$$\frac{R_H^3}{R_o^3} = \frac{W_H}{\rho_H}\frac{\rho_o}{W_o}, \tag{21}$$

or

$$\frac{R_H}{R_o} = \sqrt[3]{\frac{\rho_o}{\rho_H}\frac{W_H}{W_o}}. \tag{22}$$

(The subscript H is used to denote conditions at altitude H, the subscript o to denote sea-level conditions.) Equation 22 scales the radii at which the absolute temperatures of the shock fronts are the same. Equation 22 may be rewritten as

$$\frac{R_H}{R_o} = \sqrt[3]{\frac{P_o}{P_H}\frac{W_H}{W_o}\frac{T_H}{T_o}}.$$

The scaling to the same shock strength, P_s/P_a, is obtained from Eq 17 by dividing both sides by first P_o, and then by P_H and equating $P_s/P_o = P_s/P_H$

$$\frac{R_{H_\xi}}{R_{o_\xi}} = \sqrt[3]{\frac{P_o}{P_H}\frac{W_H}{W_o}} \tag{23}$$

This equation is currently known as Sachs' scaling law and is applicable to the shock wave at large distances from the fireball if W_H and W_o are the respective blast energies. Since $T_H < T_o$, the radius, R_H, is somewhat less than R_{H_ξ}.

If the energy encompassed by the two shock fronts is the same, Eq 22 becomes

$$\frac{R_H}{R_o} = \sqrt[3]{\frac{\rho_o}{\rho_H}}. \tag{24}$$

SC-2969

If the radii are scaled in this manner, it is seen that the total mass of air encompassed by the two shock fronts is the same and that they have the same temperature is not surprising.

If the fireball at sea level has a surface temperature T when its radius is R_o and the interior of the fireball is similar to that of Fig. 1, radii to the surface and to corresponding temperature points inside the fireball at altitude H may be scaled by use of Eq 22. If, in the expansion of the sea-level fireball by an increment dR_o, the surface temperature decreased from T to T - dT, a corresponding decrease in temperature at the higher altitude will occur over a distance dR_H.

$$\frac{dR_H}{dR_o} = \sqrt[3]{\frac{W_H}{W_o}\frac{\rho_o}{\rho_H}} . \qquad (25)$$

At the higher altitude the weapon radiates at a temperature T for a time dt_H, whereas at sea level the same weapon radiates for a time dt_o, and

$$\frac{dt_H}{dt_o} = \frac{dR_H}{\dot{R}_H}\frac{\dot{R}_o}{dR_o} = \frac{dR_H}{dR_o}$$

where $\dot{R}_H = \dot{R}_o$ since at the same absolute temperature the shock velocities are the same (Eq 15).

An Approximation of Early Thermal Radiation

<u>First Approximation</u>. -- Since at sea level the fraction of the total radiochemical yield emitted as thermal radiation during the period from zero time until the first minimum of fireball intensity is but a small percentage (about 1 per cent) of the yield, let us assume that the energy encompassed by the shock front is constant and equal to the radiochemical yield even for a detonation at altitude H. The ratio of the thermal radiation at altitude H to that at sea level is then given by Eqs 4, 24, and 26:

$$\frac{Q_H}{Q_o} = \frac{\int R_H^2 \, dR_H}{\int R_o^2 \, dR_o} = \left(\frac{\rho_o}{\rho_H}\right)^{2/3} \left(\frac{\rho_o}{\rho_H}\right)^{1/3} = \frac{\rho_o}{\rho_H} . \qquad (27)$$

Thus the amount of thermal radiation at altitude H is ρ_o/ρ_H times that at sea level if the radiation loss is assumed to be negligible for both altitudes, ie, the energy encompassed by the shock front to be constant.

Values of ρ_o/ρ_H for various altitudes are given in Table I. In view of the fact that the total radiation at sea level during this period is about 1 per cent (Q_o = 1 per cent), these values of ρ_o/ρ_H should represent approximately the percentages of the radiochemical yield radiated at altitude H during this same period. At altitudes of 20,000-30,000 feet this percentage of radiation is still a very small percentage of the radiochemical yield; but at altitudes greater than 60-thousand feet this percentage becomes a sizeable part of the radiochemical yield. Therefore the approximation that there has been a negligible change in the energy encompassed by the shock front is a poor approximation.

Second Approximation. -- It must, in the light of the preceding analysis, be concluded that for high-altitude detonations a sizeable fraction of the radiochemical yield is emitted as thermal radiation during the period from zero time until the first minimum in the fireball intensity. Therefore any method for approximating the actual thermal radiation must take into account the change in the amount of energy encompassed by the shock front during this period. Let this energy be $W_H(R)$ when the shock front is at R_H. The change in this energy, dW_H, at altitude H, compared with the change in the energy, dW_o, at sea level when the surfaces of the fireballs are at the same temperature, is

$$\frac{dW_H}{dW_o} = \frac{R_H^2\, dR_H}{R_o^2\, dR_o} = \frac{\rho_o}{\rho_H}\,\frac{W_H}{W_o}, \tag{28}$$

as is seen from combining Eqs 22 and 25. Consequently

$$\frac{\int_E^{E_H} dW_H/W_H}{\int_E^{E_o} dW_o/W_o} = \frac{\rho_o}{\rho_H}, \tag{29}$$

where E is the radiochemical yield of the weapon. E_H is the energy remaining within the shock front after thermal radiation until breakaway of the shock wave at altitude H; it is the 'apparent' yield of the weapon for the further development of the blast after breakaway of the shock wave from the fireball. E_o is the corresponding energy within the shock front at sea level at the time of breakaway and is about 0.99 E. Upon integration Eq 29 becomes

$$E_H/E = (E_o/E)^{\rho_o/\rho_H}. \tag{30}$$

Equation 30 is evaluated in Table I for various altitudes, using $E_o/E = 0.99$.

TABLE I

Results of Early Thermal Radiation

Height of burst (kft)	1st approximation $Q_H/Q_o = \rho_o/\rho_H$	2nd approximation E_H/E	Q_H/Q_o	R_H/R_o
0	1	0.990	1	1
10	1.355	0.9865	1.35	1.102
20	1.875	0.9815	1.85	1.226
30	2.68	0.973	2.7	1.377
40	4.05	0.961	3.9	1.573
50	6.58	0.9365	6.35	1.831
60	10.60	0.899	10.1	2.120
70	16.86	0.845	15.5	2.425
80	26.60	0.765	23.5	2.73
90	43.10	0.649	35.1	3.03
100	68.75	0.501	49.9	3.25

The symbols in Table I have the following definitions: E_H is the energy remaining behind the shock front at the time of breakaway of the shock wave from the fireball. Since E is the total yield of the weapon, the column E_H/E is the fraction of the yield remaining after radiation of the fireball until the time of breakaway. Q_H is the amount of thermal energy that has been radiated prior to breakaway based on assumption that the corresponding amount at sea level Q_o is 1 per cent. The ratio of the radius of the fireball R_H at the altitude H and the radius of the fireball R_o at sea level at the time of breakaway is given in the last column.

An Alternative Calculation of Early Thermal Radiation for a Detonation at 90-Thousand Feet

An alternative, though not completely independent, means for determining the amount of thermal energy radiated before breakaway of the shock wave from the fireball can be carried out at any particular altitude. Given a temperature, radius and time history of a fireball [6.6] it is of course possible to calculate the rate of radiation of the ball of fire as a function of time after the explosion [6.20]. Integration of the intensity-time plot gives the total thermal radiation emitted. To obtain a history of a fireball at a high altitude the following procedure was adopted: scale the sea level 20-KT time and radius intervals between successive temperatures to 90-thousand feet using only the change in ambient density in equations 20 and 22. During the early growth by radiation phase the

yield is still 20 KT ($W_H = W_o$). As the fireball grows by intervals of decreasing temperature, the amount of energy radiated can be computed and the yield W_H adjusted for scaling the next interval of time and radius. The rate of growth of a 20-KT fireball at 90-thousand feet was obtained (Fig. 2). At very early times, the fireball is expanding as determined by 20 KT. Near the first minimum in fireball intensity, it is expanding like a 13-KT fireball. The amount of thermal radiation that has been emitted as a function of time is given in Fig. 3. The numerical integration gave 34.2 per cent of the yield as being radiated before the first minimum in the fireball intensity. This is in good agreement with the second approximation result that 35.1 per cent was radiated before the first minimum at 90-thousand feet. The amount of energy radiated at early times and near the first minimum is very small, so the results are weakly influenced by the assumptions made in the early isothermal fireball phase of expansion and the assumed time and distance of the minimum in fireball intensity. A similar calculation can be carried at any other altitude. The assumptions in equation 30 are also implicit in the above calculations.

Partition of Energy from Nuclear Explosions and Some Results from the Variation with Altitude

During the small interval of time when the shock front and surface of the fireball coincide, an amount of energy Q_H is radiated from the shock front. The amount radiated at sea level is about 1 per cent, but, as we have seen, perhaps 50 per cent of the total yield of the weapon is radiated during this phase at 100-thousand feet. One does not expect the strength of the blast at a given distance from such a weapon to be the same as one that did not radiate. The energy remaining behind the shock front, E_H, can, to a first approximation, be expected to be partitioned as at sea level. The partition of energy at sea level results in one-third of the prompt fission energy [1.55] of the weapon being emitted as thermal radiation [6.2]. Thus, at 100-thousand feet thermal radiation accounts for two-thirds of the total yield of the weapon. In a similar manner, the partition of energy into thermal radiation can be calculated at other altitudes.

The amount of energy released as prompt gamma radiation and prompt neutrons [1.55] is independent of altitude. The ambient conditions will, however, determine their mean free paths in the atmosphere. The mean free paths are probably inversely proportional to the density. Having scaled corresponding points of the fireballs as the inverse cube root of the densities, more gamma radiation and neutrons will escape the fireballs at higher altitudes.

SC-2969

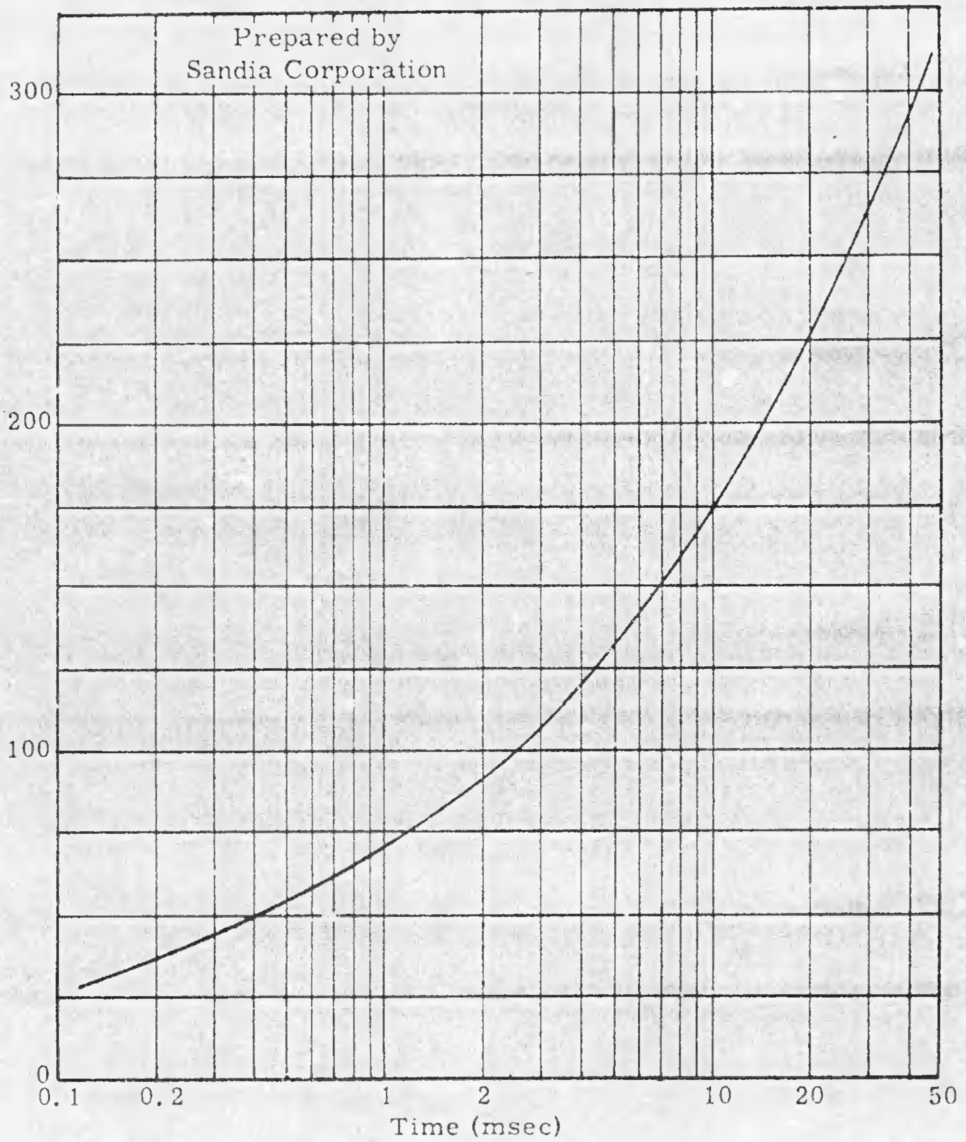

Fig. 2 -- Rate of growth of fireball for 20-KT detonation at 90-thousand feet

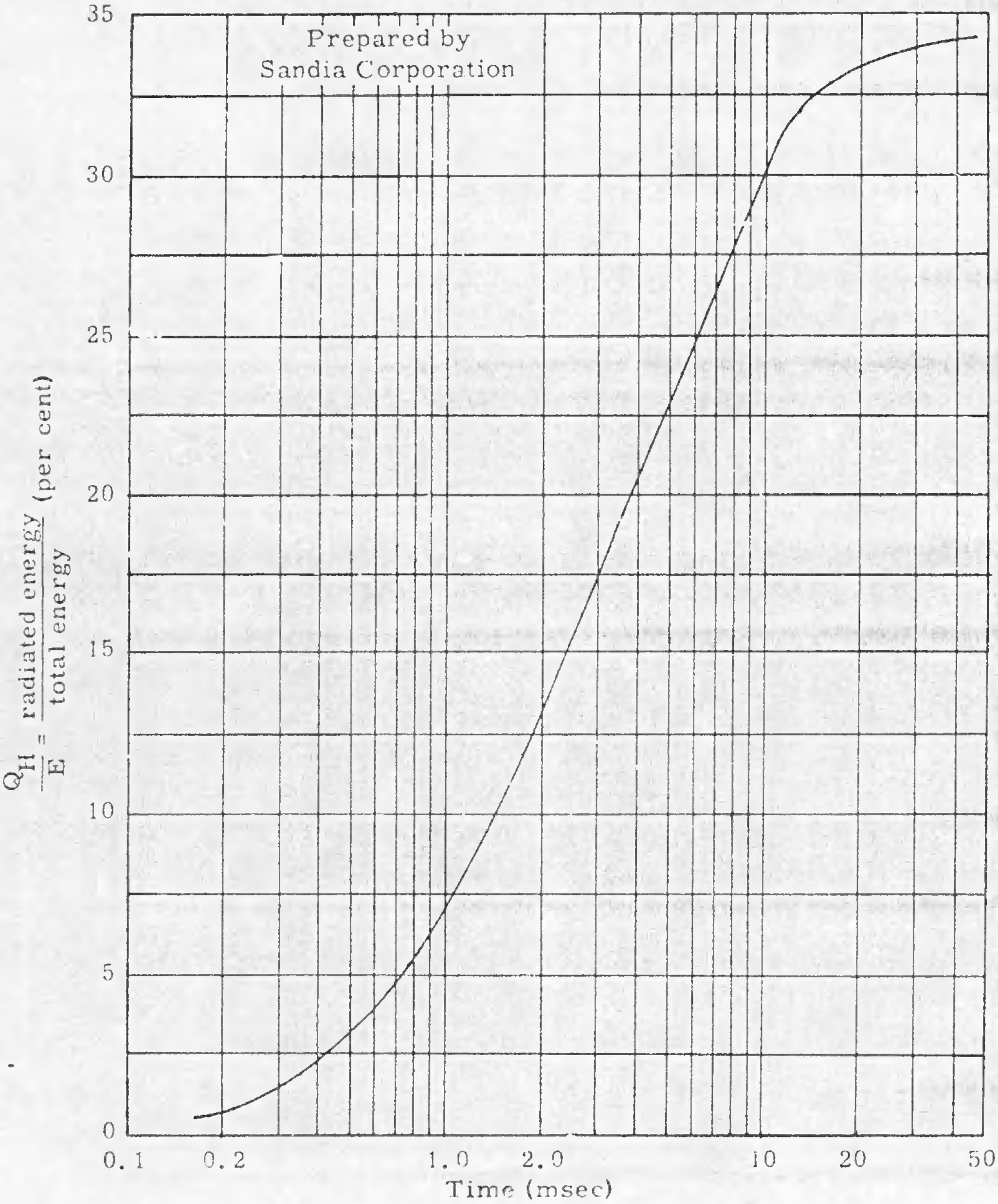

Fig. 3 -- Percentage of total energy that has been radiated as a function of time (90-thousand feet)

59-2769

The blast efficiency of a nuclear detonation is defined in terms of the weight of TNT necessary to produce the same pressure-distance values. Unfortunately, having matched the pressure-distance at say 10 psi, the same weight of TNT does not fit the nuclear pressure-distance for other pressures [3.14 and footnote]. In general, the blast efficiency of a nuclear detonation is less than that for the same energy release of TNT [3.14 footnote]. It is, however, quite easy to obviate the unfortunate definition of the blast efficiency of a nuclear weapon. Suppose the blast energy of a sea-level nuclear detonation is λE at the breakaway conditions of the shock wave. The blast efficiency factor λ is probably not known at breakaway but is less than one. Since we are partitioning the energy E_H remaining at breakaway at the altitude H in the same manner as a sea-level detonation, the blast energy of the high-altitude detonation is λE_H. Because we are always interested in scaling sea level blast results to the higher altitudes by Sachs' scaling (Eq 23) in which the ratio $\lambda E_H/\lambda E = E_H/E$ occurs, it is never necessary to know λ. The result is that the ratios of the blast energy at the high altitudes to the blast energy at sea level are simply the values E_H/E given in Table I.

SC-2969.

A detonation at 50-thousand feet results in about 6 per cent of the yield of the weapon being emitted as early thermal radiation. This means an increase of about 12 per cent in the total amount of thermal and about 6 per cent decrease in blast energy. Let us investigate the changes in radii to a given calorie level and to a given shock strength. Suppose the calorie level of interest is Q_o given by

$$Q_o = T/4\pi R^2 \tag{31}$$

where T is the total thermal energy. The radius to the given calorie level is

$$R = KT^{1/2} . \tag{32}$$

Differentiating

$$dR = \frac{1}{2} KT^{-1/2} dT \tag{33}$$

hence

$$dR/R = \frac{1}{2} dT/T . \tag{34}$$

Thus a 12 per cent change in thermal energy results in a 6 per cent change in radius to a given calorie level.

The radius to a given shock strength (P_s/P_H) at an altitude H varies (Eq 23) as

$$R_H = KW_H^{1/3} \tag{35}$$

differentiating we obtain

$$dR_H = \frac{K}{3} W_H^{-2/3} dW_H \tag{36}$$

hence

$$dR_H/R_H = \frac{1}{3} dW_H/W_H \tag{37}$$

Therefore, a 6 per cent change in the blast energy of the weapon results in a 2 per cent change in radius to a given shock strength. Early thermal radiation results in small changes in the radii to given calorie levels and shock strengths when detonations occur at altitudes less than 50-thousand feet. For detonations at altitudes less than 50-thousand feet the percentage change in constant thermal and blast radii will be less than the 6 per cent and 2 per cent obtained above.

A Discussion of the Results of the Second Approximation

The line in Table I between the altitude levels of 50-thousand and 60-thousand feet is to be interpreted as follows: at altitudes less than 50-thousand feet the amount of thermal radiation emitted during the early phase of fireball growth is small enough that conditions do not differ markedly from those for a sea-level burst. Furthermore, differences in ambient conditions are small enough to make it feasible to scale the blast and thermal energies for higher-altitude bursts from those for a similar burst at sea level. To apply Sachs' scaling for the shock strengths at large distances from the weapon, the energy should be adjusted to the value E_H/E. Table I can be used to compute the total thermal radiation from zero time until breakaway, and the time interval over which this radiation takes place may be computed from Eq 20, using the second approximation results for E_H. At altitudes greater than 60-thousand feet, however, it is evident from the second approximation that changes in ambient conditions cause serious deviations in the total thermal radiation emitted during this initial period as compared with that emitted at sea level.

SC-2767

The aim of this analysis was to obtain approximations of emitted thermal radiation for all burst altitudes and determine at what altitude range serious deviations from that for sea-level detonations takes place. Table I summarizes the results of this analysis in that the values for total radiation emitted at altitudes less than 50-thousand feet are thought to be essentially correct, whereas those for altitudes greater than 60-thousand feet are subject to a number of influencing factors. The most serious factor is probably

the increased thermal radiation from the shock front, resulting in a dissipation of the shock pressure, P_s, near the front. At a lower-pressure front than expected the amount of thermal radiation that can be emitted would be lessened. On the other hand, the mean free paths of radiation should be longer at lower densities, and hence at higher altitudes radiation could be emitted from greater depths, ie, higher temperatures, behind the shock front. Estimation of the extent to which these two effects compensate each other has not been attempted. Because the radiation-transfer phase of the nuclear explosion is not governed by hydrodynamic laws, any scaling law based on hydrodynamic considerations will not scale the growth of the fireball in its entirety. Although hydrodynamic scaling laws have been applied in this paper, the early phase of radiation transfer contributes only a small fraction of the radiation which escapes the fireball prior to breakaway of the shock wave. Scaling the radiation-transfer phase hydrodynamically should not, therefore, cause a significant error compared with other sources of error.

Radii, R_H, of the fireballs at various altitudes are presented in Table I, expressed as ratios to the corresponding radius, R_o, at sea level. These radii were calculated from Eq 22 by substituting E_H/E, as determined from the second approximation, for W_H/W_o. For example, the radius of the fireball for a 20-KT weapon at breakaway is about 330 feet at sea level; this fireball continues to grow until it finally attains a radius of about 450 feet. At 100-thousand feet this weapon will have a radius of about 1,070 feet at breakaway and attain a final radius of about 1,465 feet. The final radius at 100-thousand feet is about the same as the corresponding radius for a fireball from a 700-KT weapon burst at sea level. Thus, in view of the differences in spherical surface area and the fact that radiation is essentially a surface phenomenon, radiation increases as the square of these radii.

SC-2969

The amount of energy radiated during the first thermal pulse (from zero time to the first minimum of fireball intensity) at very high altitudes (of the order of 90-thousand feet) is about the same as that emitted during the second thermal pulse (from the first minimum through the second maximum until the fireball is extinguished) at sea level. The times during which the thermal radiation at various altitudes is emitted are, of course, much different. Suppose the average intensity of the thermal pulse is dQ_o/dt_o at sea level (the thermal pulse through the second maximum). This radiation takes place over about 3 sec Fig. [6.20] for a 20-KT weapon at sea level while the same amount of energy is delivered in 0.044 second during the first thermal pulse at 90-thousand feet. Thus the average intensity of early thermal radiation at 90-thousand feet is about 70 times that of the total thermal pulse at sea level. If this thermal emission is viewed

from the standpoint of damage, because the first thermal pulse at the high altitude is emitted in a short time, temperatures upon absorbing surfaces can be expected to be very large. Use of total calories incident upon a surface would, at the high altitude, be a poor criterion of thermal damage. Because the area of the fireball is so much larger at the higher altitudes, the second thermal pulse can also be expected to have a shorter duration. The second pulse can be emitted as soon as the blanketing nitrogen compounds have been dissociated, and it may occur while the shock front is still near the surface of the fireball. Rapid emission of radiation from the fireball at this point may cause a premature negative phase of the shock wave and thus dissipate energy from the positive phase.

To recapitulate, then, at altitudes less than 50-thousand feet early thermal radiation and partition of energy into thermal and blast do not seem to be significantly different than at sea level, and appropriate scaling laws may be applied to correlate the pertinent parameters at various altitudes ranging from zero to 50-thousand feet. Corresponding blast parameters may be obtained by applying Sachs' scaling law after the yield has been adjusted in accordance with the values given in Table I under the second approximation.

At altitudes greater than 50-thousand feet, on the other hand, thermal emission during the early phase is becoming so large a percentage of total yield that some errors can be expected in scaling the sea-level phenomena even when a varying yield is taken into account. Table I illustrates the general trend of energy partition with increasing altitude. Because of the increased amount of radiation emitted within a comparatively short time interval, high intensities are expected. Likewise corresponding temperatures of material surfaces at the same calorie level should increase greatly for bursts at higher altitudes. And significant, also, is the fact that the amount of energy going into blast is decreasing rapidly with increasing heights of burst above 50-thousand feet.

The Variation of Lethal Radii with Altitude

Effects of nuclear weapons can conveniently be separated into those emitted by the weapon and those produced on the target. The important effects parameters are blast, thermal radiation, and prompt gamma rays. Preceding sections of this paper have been devoted to the variation in the emitted effects as a function of altitude. The importance of any variation in the partition of energy among the effects parameters is the resulting

change in lethal radii. In the investigation of lethal radii with altitude, a serious difficulty arises. It is essentially the fact that the lethal values of the parameters for a manned aircraft which flies below 50-thousand feet are most certainly not the same as the lethal values for a missile at 80-thousand feet. Because the decrease in blast efficiency with altitude gives an increase in thermal radiation, it is not readily apparent what this means in regard to the lethal radii.

Lacking better information, fixed values for the lethal overpressure, gust, thermal radiation, and gamma radiation were chosen. The lethal values are reasonably close to those for present day aircraft such as the B-29 and were used in the curves prepared in a previous paper.[9]

Lethal values:

6 psi overpressure (ΔP)
0.3 psi dynamic pressure (q) (130-mph wind at sea level)
60 cal/cm^2 thermal radiation (Q)
5000 Roentgen gamma radiation (γ) for personnel

Using the variation with altitude of the partition of blast and thermal energy as derived in the preceding sections lethal radii for several yields are presented as a function of altitude (Figs. 4 and 5).

Below an altitude of 50-thousand feet, if the calculations of early thermal radiation have been 100 per cent in error, this still would represent only insignificant changes in the curves. The variation from sea-level values of the blast energy caused by new ambient conditions are about 6 per cent at 50-thousand feet. If the sea-level partition of energy were used at 50-thousand feet the gust curves would be at radii 2 per cent greater than the plotted values. The thermal lethal radii have been increased 6 per cent more than those given by a sea-level partition of energy at 50-thousand feet. At altitudes below 50-thousand feet, the percentages are smaller. The variation in the blast energy and thermal radiation over the first 50-thousand feet in altitude are probably the order of instrumentation errors. For a 1-KT weapon detonated at 50-thousand feet, the lethal gust radius has been decreased only 30 feet and the lethal thermal radius increased 45 feet due to the variation in the partition of energy from a sea-level condition. Scaling the results of a sea-level detonation to 50-thousand feet are apt to be more accurate than the instrumentation of a detonation at 50-thousand feet. If the targets are individual flying aircraft, the lethal radii for even a 1-KT weapon are so large (greater than 760 feet) that the fuzing requirements to assure enclosure of the aircraft in a lethal envelope

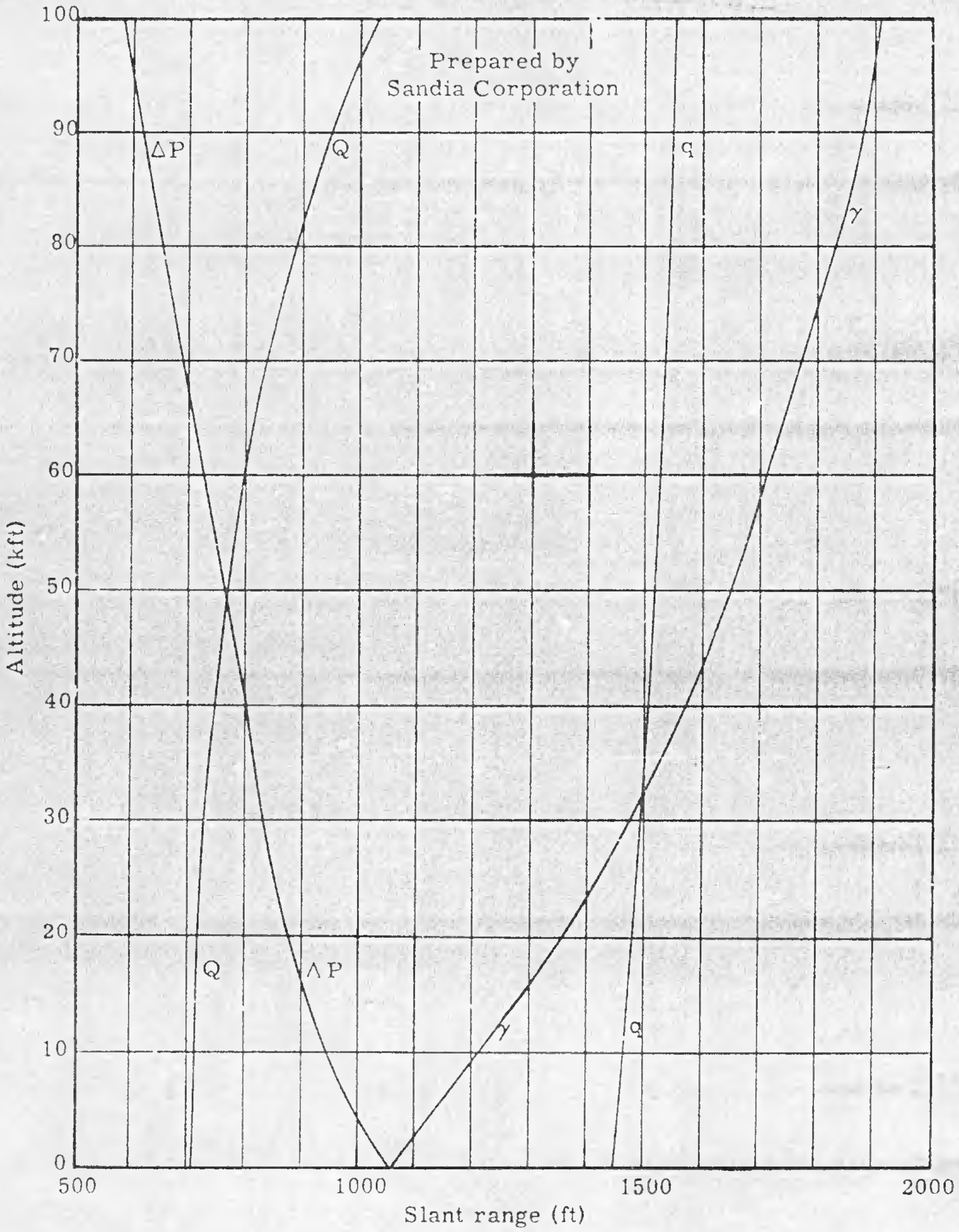

Fig. 4 -- Variation of lethal radii with altitude for a 1-KT weapon

SC-2969

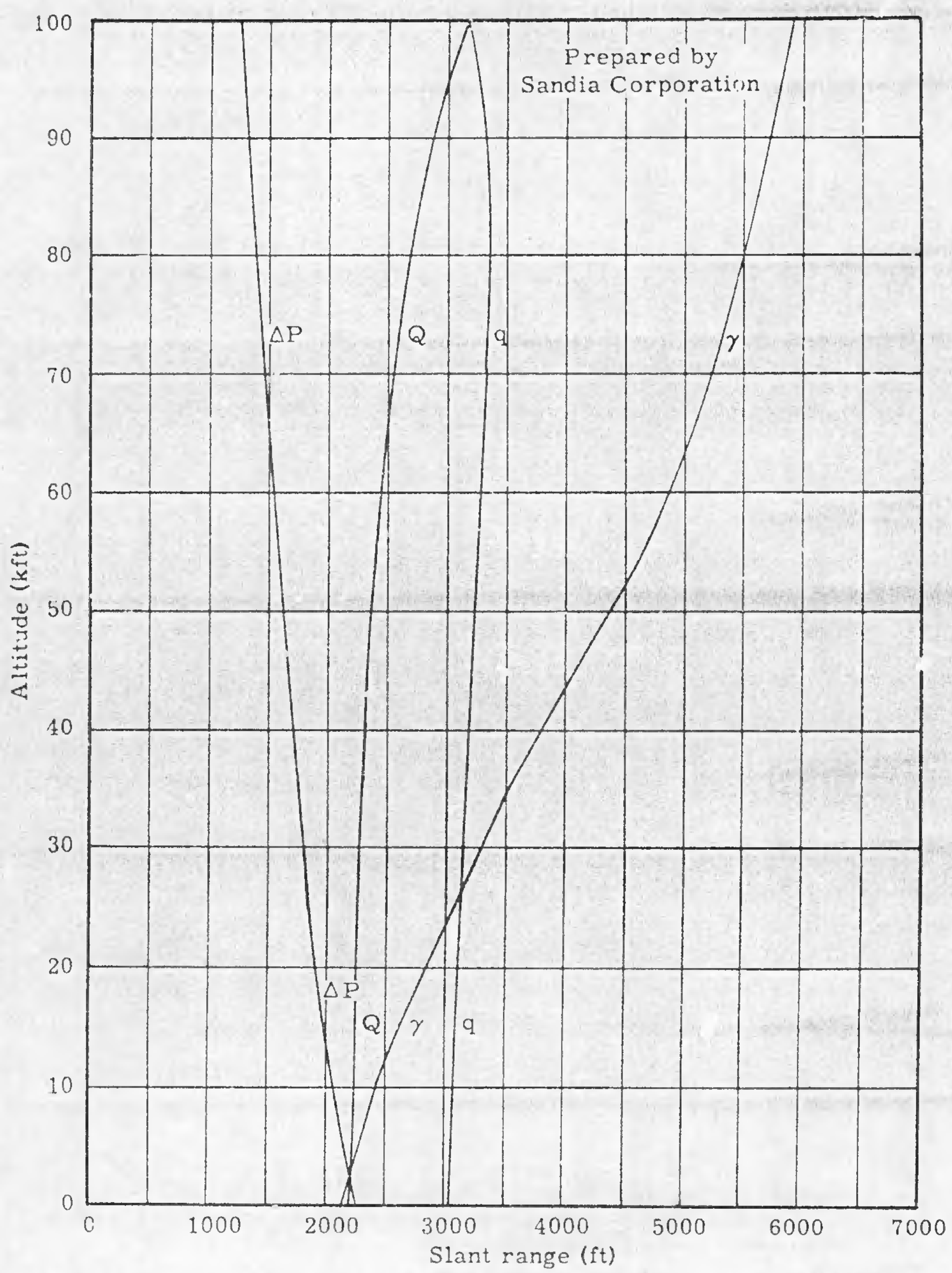

Fig. 5 -- Variation of lethal radii with altitude for a 10-KT weapon

[redacted]

UNCLASSIFIED

are not stringent. The variation of partition of energy into blast and thermal radiation below 50-thousand feet would appear to be an academic rather than a practical subject.

Above 50-thousand feet altitude, where the calculated variation in partition of energy becomes important, three of the effects parameters Q, q, and γ have generally increasing lethal radii with altitude. Above 50-thousand feet, the fuzing requirements are becoming less severe than below 50-thousand feet to obtain the <u>same</u> lethal values of the damaging parameters. Any other than the above calculated partition of energy will shift either the thermal (Q) or dynamic pressure (q) curve out to a larger lethal radius and leave the gamma radiation curves unchanged. This is nicely illustrated for the 10-KT weapon detonated at 100-thousand feet. Any other partition of energy would have resulted in either Q, or q at a larger lethal radius for the weapon. For yields larger than 10 KT, the variation in partition of energy results in the lethal radius for thermal radiation (Q) exceeding the dynamic pressure (q) lethal radius. Gamma radiation is a lethal parameter only so long as the target is occupied by personnel. Because missiles that fly at 80-thousand feet will have much different structure than conventional aircraft, the necessary lethal dynamic pressures will be much larger than those assumed above. Indeed, the targets may be so 'hard' that the lethal criterion will be thermal radiation. Such being the case, the variation in the partition of energy giving an increased thermal radiation in a very short time may mean the nuclear device is more efficient than had no variation in the partition of energy taken place. The important unknowns are not in the emitted effects of nuclear weapons, rather the unknowns are the targets and the effects of nuclear weapons upon these targets.

[redacted]

UNCLASSIFIED

LIST OF REFERENCES

1. The Effects of Atomic Weapons (Prepared under the direction of the Los Alamos Scientific Laboratory), McGraw-Hill, New York, 1950

2. Private communication from J. O. Hirschfelder, University of Wisconsin

3. Cole, R. H., Underwater Explosions, Princeton University Press, Princeton, New Jersey, 1948

4. Fuchs, K., and Peierls, R., The Equations of State of Air, Los Alamos Scientific Laboratory report, April 2, 1947 (Unclassified)

5. Schneider, E. G., "Absorption Data," J. Opt. Soc. Am. 30, 128 (1940)

6. Courant, R., and Friedrichs, K. O., Supersonic Flow and Shock Waves, Interscience Publishers, New York, 1948

7. Blast Wave (Ed by H. A. Bethe), Vol 7, Part II, Los Alamos Scientific Laboratory report LA-1021, August 13, 1947 (Secret)

8. Hirschfelder J., and Curtiss W. E., Thermodynamic Properties of Air, University of Wisconsin Press, Madison, Wisconsin, (1948)

9. Cook, T. B., Jr., Broyles, C. D., and Shelton, F. H., Preliminary Curves of Atomic Weapons Effects for Burst Altitudes from Sea Level to 100,000 Feet, Sandia Corporation Technical Memorandum 97-53-51, July 21, 1953 (Secret)

SC-2969

INITIAL DISTRIBUTION

1 R. E. Poole, 1000
2 W. A. MacNair, 5000
3 R. W. Henderson, 1200
4 L. A. Hopkins, 1300
5 L. J. Paddison, 1500
6 S. C. Hight, 5100
7 G. A. Fowler, 5200
8 F. J. Given, 5300
9 L. G. Abraham, 5400
10 W. J. Howard, 1330
11 E. F. Cox, 5110
12 K. W. Erickson, 5130
13 G. E. Hansche, 5140
14 M. L. Merritt, 5111
15 G. T. Pelsor, 5121
16 W. E. Boyes, 5131
17 S. H. Dike, 5133
18 Dr. Alvin C. Graves, LASL
19 Dr. John von Neumann, IAS, Princeton
20 Dr. Walker Bleakney, Princeton University
21 Dr. C. W. Lampson, BRL
22 Dr. G. K. Hartmann, NOL
23 Prof. H. C. Hottel, MIT
24 Dr. Fred Reines, LASL
25 Mr. F. B. Porzel, LASL
26 Dr. W. E. Ogle, LASL
27 Dr. H. W. Bode, BTL
28 Dr. R. F. Bacher, CIT
29 Dr. E. B. Doll, SRI
30 Dr. M. V. Barton, University of Texas
31 Dr. Paul Fine, DMA/AEC
32-34 DMA/AEC Classified Document Room
35 AEC Technical Information Service, Oak Ridge, Tennessee
192-210 Sandia Corporation Document Division

(Through AFSWP/FC)

ARMY

36 Asst Chief of Staff, G-2, D/A, Washington 25, DC
37 Asst Chief of Staff, G-3, D/A, Washington 25, DC, ATTN: DACofS, G-3, (RR&SW)
38 Asst Chief of Staff, G-4, D/A, Washington 25, DC
39 Chief of Ordnance, D/A, Washington 25, DC, ATTN: ORDTX-AR
40-42 Chief Signal Officer, D/A, P&O Division, Washington 25, DC, ATTN: SIGCP
43-44 Chief Chemical Officer, D/A, Washington 25, DC

INITIAL DISTRIBUTION (cont)

45 The Quartermaster General, CBR, Liaison Office, Research and Development Division, D/A, Washington 25, DC
46-48 Chief, Army Field Forces, Ft Monroe, Va
49 Army Field Forces Board No. 4, Ft Bliss, Tex
50 Commandant, Command and General Staff College, Ft Levenworth, Kan ATTN: ALLIS(AS)
51 Commandant, The Artillery School, Ft Sill, Okla
52 Commandant, The AA &GM Branch, The Artillery School, Ft Bliss, Tex
53 The Superintendent, US Military Academy, West Point, NY, ATTN: Prof of Ord
54 Commanding General, Research and Engineering Command, Army Chemical Center, Md, ATTN: Special Projects Officer
55-56 RD Control Officer, Aberdeen Proving Grounds, Md, ATTN: Director, Ballistics Research Laboratory
57 Commanding Officer, Engineer Research and Development Laboratory, Ft Belvoir, Va, ATTN: Chief, Technical Intelligence Br
58 Chief, Quartermaster R&D Laboratory, Philadelphia Quartermaster Depot, Philadelphia 45, Pa, ATTN: Mr. John Davis
59 Director, Operations Research Office, Johns Hopkins University, 6410 Connecticut Ave, Chevy Chase, Md, ATTN: Library
60 Director, Special Weapons Development, OCAFF, Ft Bliss, Tex
61 Director, Technical Documents Center, Evans Signal Laboratory, Belmar, NJ

SC-2969

NAVY

62-63 Chief of Naval Operations, D/N, Washington 25, DC, ATTN: Op-36
64-65 Chief, Bureau of Medicine and Surgery, D/N, Washington 25, DC, ATTN: Special Weapons Defense Div
66 Chief, Bureau of Ordnance, D/N, Washington 25, DC
67 Chief, Bureau of Ships, D/N, Washington 25, DC, ATTN: Code 348
68-69 Chief, Bureau of Aeronautics, D/N, Washington 25, DC
70 Chief of Naval Research, D/N, Bldg T-3, Washington 25, DC, ATTN: Code 219, RD Control Officer
71-72 Commander, Operation Development Force, U. S. Atlantic Fleet, U. S. Naval Base, Norfolk 11, Va, ATTN: Tactical Development Group; Air Department
73 President, US Naval War College, Newport, Rhode Island
74 Superintendent, USN Postgraduate School, Monterey, Calif
75-76 Commanding Officer, Fleet Training Center, Naval Base, Norfolk 11, Va, ATTN: Special Weapons School
77-78 Commanding Officer, Fleet Training Center (SPWP School) Naval Station, San Diego 36, Calif
79 Commanding Officer, Naval Damage Control Training Center, USN Base, Philadelphia 12, Pa, ATTN: ABC Defense Course
80-81 Commander, USN Ordnance Laboratory, Silver Springs 19, Md, ATTN: EE and DR
82 Commander, USN Ordnance Test Station, Inyokern, China Lake, Calif
83-84 Officer-in-Charge, USN Civil Engineering Research and Evaluation Laboratory, Construction Battalion Center, Port Hueneme, Calif, ATTN: Code 753
85 Commanding Officer, USN Medical Research Institute, National Naval Medical Center, Bethesda 14, Maryland

UNCLASSIFIED

INITIAL DISTRIBUTION (cont)

86 Director, USN Research Laboratory, Washington 25, DC, ATTN: Dr. E. O. Hulburt
87 Commanding Officer and Director, USN Electronics Laboratory, San Diego 52, Calif, ATTN: Code 210
88-89 Commanding Officer, USN Radiological Defense Laboratory, San Francisco, Calif, ATTN: Technical Information Division
90 Commander, Naval Air Development Center, Johnsville, Pa
91 Director, Material Laboratory, New York Naval Shipyards, Brooklyn 1, NY

OTHERS

92 Executive Secretary, Joint Chiefs of Staff, Washington 25, DC
93 Director, Weapons Systems Evaluation Group, OSD, Rm 2E1006, Pentagon, Washington 25, DC
94 Executive Secretary, Military Liaison Committee, PO Box 1814, Washington 25, DC
95 Commandant, National War College, Washington 25, DC, ATTN: Classified Records Section, Library
96-135 Commanding General, Field Command, AFSWP, PO Box 5100, Albuquerque, NM
136-144 Chief, AFSWP, PO Box 2610, Washington 13, DC
145 National Advisory Committee for Aeronautics, 1724 F St, NW, Washington, DC, ATTN: Materials Research Coordination Group
146 Dr. David T. Griggs, Institute of Geophysics, University of California, Los Angeles 24, Calif

SC-2967

(Through AFSWC)

AIR FORCE

147 Asst for Atomic Energy, Hqs, USAF, Washington 25, DC, ATTN: DCS/O
148-149 Asst for Development Planning, Hqs, USAF, Washington 25, DC
150 Director of Operations, Hqs, USAF, Washington 25, DC, ATTN: Operations Analysis
151 Directorate of Requirements, Hqs, USAF, Washington 25, DC, ATTN: AFDRQ-SA/M
152 Directorate of Research and Development, Armament Div, DCS/D, Hqs, USAF, Washington 25, DC
153-154 Directorate of Intelligence, Hqs, USAF, Washington 25, DC, ATTN: AFOIN-1B2
155 Commanding General, Strategic Air Command, Offutt AFB, Omaha, Nebr, ATTN: Chief, Operations Analysis
156-158 Commanding General, Tactical Air Command, Langley AFB, Va, ATTN: Document Security Br
159 Commanding General, Air Defense Command, Ent AFB, Colo ATTN: ADMAR-2
160-161 Commanding General, Air Materiel Command, Wright-Patterson AFB, Dayton, Ohio
162-164 Commanding General, Air Research and Development Command, PO Box 1395, Baltimore 3, Md, ATTN: RDDN
165-166 Commandant, Air Command and Staff School, Maxwell AFB, Ala
167-169 Commanding General, Wright Air Development Center, Wright-Patterson AFB, Dayton, Ohio, ATTN: WCOESP

UNCLASSIFIED

UNCLASSIFIED

INITIAL DISTRIBUTION (cont)

170-171 Commanding General, AF Cambridge Research Center, 230 Albany St, Cambridge 39, Mass, ATTN: Atomic Warfare Directorate CRTSL-2

172-186 Commanding General, Air Force Special Weapons Center, Kirtland AFB, NM, ATTN: Chief, Tech Lib Br

187-189 Commanding General, 1009th Special Weapons Squadron, 1712 G St, NW, Washington 25, DC

190-191 The RAND Corporation, 1700 Main Street, Santa Monica, Calif, ATTN: Nuclear Energy Division

SC-2969

UNCLASSIFIED